SUPPLEMENTARY INFORMATION

Design of a single-chain polypeptide tetrahedron assembled from coiled-coil segments

Helena Gradišar[1,2], Sabina Božič[1], Tibor Doles[1,2], Damjan Vengust[3], Iva Hafner-Bratkovič[1], Alenka Mertelj[3,4], Ben Webb[5–7], Andrej Šali[5–7], Sandi Klavžar[4,8] & Roman Jerala[1,2,9]*

[1]Department of Biotechnology, National Institute of Chemistry, Ljubljana, Slovenia. [2]Excellent NMR–Future Innovation for Sustainable Technologies Centre of Excellence, Ljubljana, Slovenia. [3]Jožef Stefan Institute, Ljubljana, Slovenia. [4]Faculty of Mathematics and Physics, University of Ljubljana, Ljubljana, Slovenia. [5]Department of Bioengineering and Therapeutic Sciences, University of California–San Francisco, San Fransisco, USA. [6]Department of Pharmaceutical Chemistry, University of California–San Francisco, San Fransisco, USA. [7]California Institute for Quantitative Biosciences, University of California–San Francisco, San Fransisco, USA. [8]Faculty of Natural Sciences and Mathematics, University of Maribor, Maribor, Slovenia. [9]Faculty of Chemistry and Chemical Technology, University of Ljubljana, Ljubljana, Slovenia.

***Correspondence** should be addressed to Roman Jerala, Department of Biotechnology, National Institute of Chemistry, Hajdrihova 19, SI-1000 Ljubljana, Slovenia.
tel. no.: +38614760335, fax: +38614760300, email: roman.jerala@ki.si

Supplementary results contain:

- **Supplementary note (1)**
- **Supplementary tables (2)**
- **Supplementary figures (1-11)**

Nature Chemical Biology: doi:10.1038/nchembio.1248

SUPPLEMENTARY RESULTS

Supplementary Note 1 | Mathematical analysis of the polyhedral topologies composed of a single chain.

Suppose a polyhedron *P* is composed of a single polymer chain. Then *P* can be naturally represented with the digraph *D(P)* whose vertices are the end-points of segments and its arcs follow the orientations of the segments. Since the arcs of *D(P)* appear in pairs, *D(P)* is an Eulerian digraph, moreover, the segments of the polymer chain correspond to an Eulerian tour *T* in *D(P)*. In order for *P* to be stable, *T* must fulfill the following conditions for every vertex *u* of *D(P)*:

(i) after *T* enters *u* from a vertex *v*, it does not immediately continue (return) to *v*;
(ii) after *T* passes *u* as $v \to u \to w$, it later neither passes *u* as $v \to u \to w$ nor as $w \to u \to v$.

Conditions (i) and (ii) are illustrated in **Supplementary Fig. 1**.

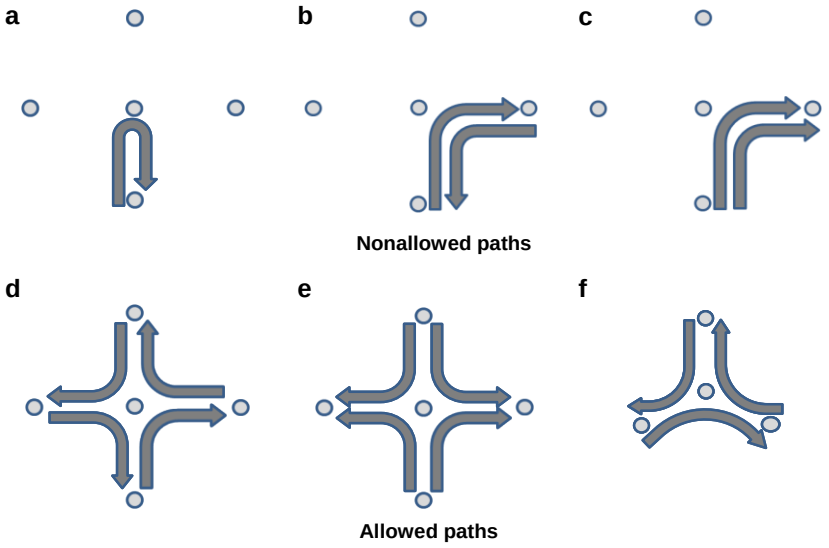

Supplementary Figure 1 | Constraints for allowed types of vertices for stable polyhedra. (**a-c**) Non-allowed paths that lead to the unstable vertex, shown in an example of a vertex with 4 converging edges, which is also relevant for vertices of other types. This type of connection does not lock all paths of the vertex. (**d-f**) Examples of two types of allowed connections in the vertices converging four (**d,e**) and three edges (**f**).

If (i) and (ii) hold for a vertex *u* we say that *u* is *stable* (with respect to *T*). If every vertex of *D(P)* is stable (with respect to *T*) then *T* is called *stable*. Hence a realization of a polyhedron *P* with a single polymer chain corresponds to a stable Eulerian tour in *D(P)*.

Let now *G* be an arbitrary connected graph. Then the *double of G* is the graph *G'* obtained from *G* by replacing each of its edges with two parallel edges. Such a pair of edges will be called a *double edge*. Call a graph *G realizable* (with a single-chain self-assembling

Nature Chemical Biology: doi:10.1038/nchembio.1248

polypeptide) if its double *G'* contains a stable Eulerian tour. We point out that an Eulerian tour *T* is completely defined with the sequence of its edges. That is, a start (and an end) of *T* is not considered as a property of *T*. With this convention, condition (i) implies that the arc corresponding to the first segment of a polymer chain and the arc corresponding to its last segment must not be on the same double edge.

If *G* contains a vertex of degree 1 or a vertex of degree 2, then it is not realizable. Hence we next look to *cubic graphs*, that is the graphs whose every vertex is of degree 3, so that every vertex of the double of *G* is of degree 6. (Note that the tetrahedron is the smallest cubic graph.) For a cubic graph, a test whether it is realizable can be simplified using the following observation.

Lemma 1: Let *T* be an Eulerian tour in the double of a graph *G* and let *u* be a vertex of degree 3 in *G*. Then *u* is stable (w. r. t. *T*) if and only if (i) is fulfilled for *u*.

Proof: We only need to show that (ii) holds for *u* provided (i) is true. Suppose on the contrary that (ii) does not hold. Then together with subsections $v \to u \to w$, the tour *T* either contains the subsection $v \to u \to w$ once more or the subsection $w \to u \to v$. Since *u* is of degree 3 in *G*, and hence of degree 6 in the double of *G*, *T* must enter *u* once more, say from *x*. But then, since all the other edges are already used, *T* must return to *x*, a contradiction with the assumption that (i) holds for *u*.

Using Lemma 1 we next prove that every cubic graph (in particular every cubic polyhedron) is realizable.

Theorem 1: All connected cubic graphs are realizable.

Proof: Let *G'* be the double of *G*. Let *m* be the number of edges of *G*, so that *G'* has 2*m* edges. Call consecutive arcs of an Eulerian tour that traverse the edges of a double edge one after the other a *bad pair*. By Lemma 1 it suffices to prove that *G'* admits an Eulerian tour with no bad pair. Since every vertex of *G'* is even (of degree 6), *G'* contains an Eulerian tour. Select an arbitrary tour in *G'*, say

$$T = v_1 \to v_2 \to \cdots \to v_{2m} \to v_1$$

and let *s* be the number of bad pairs of *T*. If $s = 0$, there is nothing to be proved. Hence suppose that $s \geq 1$. We may without loss of generality assume (because we can start the tour in any vertex) that *T* begins with $v_1 \to v_2 \to v_3 = v_1 \to \cdots$. Select an index *i* such that $v_i = v_2$ and such that $i \geq 3$ is as small as possible. Note that such an index exists because the degree of v_2 is at least 2. Observe also that $i \geq 5$ and that $v_{i+1} \neq v_1, v_2$. Consider now the sequence

$$T' = v_1 \to v_2 \to v_{i-1} \to v_{i-2} \to \cdots \to v_4 \to v_1 \to v_2 \to v_{i+1} \to v_{i+2} \to \cdots \to v_{2m} \to v_1.$$

It is straightforward to see that *T'* is an Eulerian tour in *G'*. The bad pair $v_1 \to v_2 \to v_3 = v_1$ of *T* is no longer a bad pair in *T'*. Moreover, the second arc $v_1 \to v_2$ does not form a bad pair with $v_2 \to v_{i+1}$ as well as not the arcs $v_4 \to v_1$ and $v_1 \to v_2$. Any other bad pair of *T'* corresponds to a bad pair in *T*. It follows that T' has at most $s-1$ bad pairs. Repeating the procedure we end up with an Eulerian tour with no bad pair.

We now treat stable Eulerian tours in the key object of this paper, the tetrahedron.

Nature Chemical Biology: doi:10.1038/nchembio.1248

Theorem 2: Up to symmetries, the double of the tetrahedron admits exactly three stable Eulerian tours. More precisely, the tetrahedron can be composed from a single polymer chain in exactly one of the following three ways (**Supplementary Fig. 2**):

(i) 1, 2, 3, 1, 2, 4, 3, 1, 4, 3, 2, 4, 1
(ii) 1, 2, 3, 1, 2, 4, 3, 2, 4, 1, 3, 4, 1
(iii) 1, 2, 4, 1, 2, 3, 4, 1, 3, 2, 4, 3, 1.

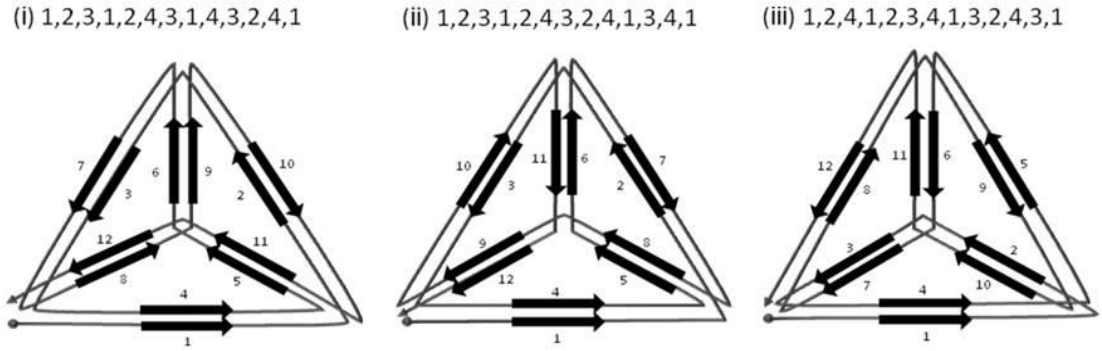

Supplementary Figure 2 | Topological solutions of self-assembling tetrahedron from a single polypeptide chain. A tetrahedron can be composed from a single polymer chain in exactly one of the three illustrated ways. We designed the polypeptide chain TET12 according to the topology (i).

Proof: Let *T* be the graph of the tetrahedron. We need to classify the stable Eulerian tours in its double *T'*. To do it, recall that by Lemma 1 we only need to check condition (i) for the vertices of *T'*. Since *T'* is a 6-regular graph, an Eulerian tour in *T'* enters (and exits) each of its vertices three times. Therefore, only two types of vertices are possible (**Supplementary Fig. 3**):

P2A – combining two parallel and one antiparallel segments
A3 – combining three antiparallel segments.

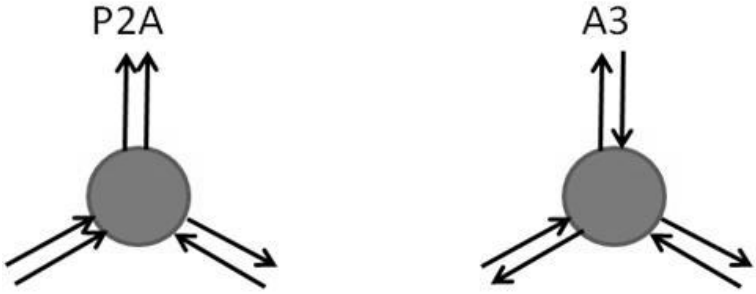

Supplementary Figure 3 | Two types of vertices existing in a cubic polyhedron. The number of incoming and outcoming helices have to be equal.

Denote the vertices of *T* (and hence also of *T'*) with 1, 2, 3, 4, and let *D* be a stable Eulerian tour. It is not difficult to see that there are only three possibilities for vertices: there are four A3 vertices, there are four P2A vertices, or there is one A3 and three P2A vertices. We treat them one by one.

Nature Chemical Biology: doi:10.1038/nchembio.1248

Case 1: All the vertices are A3.

Suppose first that *D* contains a cycle of length 3. By symmetry, we may assume that *D* starts with 1, 2, 3, 1. Since vertex 1 is of type A3, we necessarily have *D* = 1, 2, 3, 1, 4, … In the first subcase assume *D* continues to 2. Then, having in mind that all vertices are A3 and that *D* has no bad pair, we must necessarily have *D* = 1, 2, 3, 1, 4, 2, 1 3, … Continuing with 4, the vertex 1 would be a dead end, hence we necessarily have *D* = 1, 2, 3, 1, 4, 2, 1 3, 2, 4, 3, 4, …, a contradiction as *D* contains a bad pair. In the second subcase assume *D* continues to 3. Then *D* = 1, 2, 3, 1, 4, 3, 2, … If *D* continues to 1, then *D* = 1, 2, 3, 1, 4, 3, 2, 1, 3, 4, 2, 4, …, a contradiction, while if *D* continues to 4, then *D* = 1, 2, 3, 1, 4, 3, 2, 4, 1, 3, 4, 2, 1. But now the first and the last arc of *D* form a bad pair.

Suppose that *D* contains no cycle of length 3. Then we may assume that D starts with 1, 2, 3, 4, 1. Then *D* = 1, 2, 3, 4, 1, 3, 2, … *D* cannot continue with 1 because it has no 3-cycle, hence *D* = 1, 2, 3, 4, 1, 3, 2, 4, 3, …, so we have found a 3-cycle.

We have thus proved that *D* cannot contain only type A3 vertices.

Case 2: All the vertices are P2A.

As in Case 1, it is easy to argue that *D* has at least one cycle of length 3. Hence, by symmetry, we may assume that *D* starts with 1, 2, 3, 1. If *D* continues with 2, then by case analysis we infer that *D* must necessarily be:

(a) 1, 2, 3, 1, 2, 4, 3, 1, 4, 3, 2, 4, 1

In the case when If *D* continues with 4, case analysis shows that *D* is one of the following:

(b) 1, 2, 3, 1, 4, 3, 1, 2, 4, 3, 2, 4, 1
(c) 1, 2, 3, 1, 4, 3, 2, 4, 1, 2, 4, 3, 1
(d) 1, 2, 3, 1, 4, 3, 2, 4, 3, 1, 2, 4, 1.

Apply the permutation (1 2 4 3) to (b) and perform a corresponding shift to find out that (b) is the same (up to symmetries) stable Eulerian tour. Similarly, apply (1 3 4 2) to (c) and (1 4)(2 3) to (d) to conclude that also (c) and (d) are the same as (a). This case thus gives us (i).

Case 3: One vertex is A3, three vertices are P2A.

It is again not difficult to see that *D* contains at least one 3-cycle. Suppose first that *D* does not contain the cycle on vertices 1, 2, 4. Then we may assume that D starts with 1, 2, 3, 1. But then it must continue with 2, 4. Moreover, by the case assumption, the next vertex is 3, and all the rest is fixed. We conclude that *D* is necessarily

(a) 1, 2, 3, 1, 2, 4, 3, 2, 4, 1, 3, 4, 1.

This gives the tour (ii). Assume next that *D* starts with 1, 2, 4, 1. Then case analysis gives us the following two possibilities:

(b) 1, 2, 4, 1, 2, 3, 4, 1, 3, 2, 4, 3, 1
(c) 1, 2, 4, 1, 3, 2, 4, 3, 1, 2, 3, 4, 1.

Apply the permutation (1 2 4)(3) to (c) and a corresponding shift to get that (b) and (c) are the same (up to symmetries) tours and we have found the tour (iii).

To conclude the proof note that (i) is clearly different from (ii) and from (iii) since (i) was obtained in a different case than (ii) and (iii). Finally, (ii) is different from (iii) because the Eulerian tour (iii) contains a cycle consisting of three consecutive vertices - the cycle 1, 2, 4, 1 – all of which double edges are parallel. There is no such cycle in the Eulerian tour (ii).

In order to predict applicability of our approach beyond the tetrahedron (alias triangular pyramid), we computed the number of stable Eulerian tours in the double of several additional, potentially interesting polyhedra: the square pyramid, the triangular bipyramid,

Nature Chemical Biology: doi:10.1038/nchembio.1248

the triangular prism, the square prism (alias cube), and the square bipyramid (alias octahedron). In order to support our theoretical approach, computations were performed also on the double of the triangular pyramid. All enumerations were done with respect to the symmetries of the corresponding polyhedron. The obtained results are collected in **Supplementary Table 1**, where (i) and (ii) denote the two defining conditions for stable Eulerian tours and the symbols A and P indicate that Eulerian tours have only antiparallel and parallel segments, respectively. Hence the last two columns list the number of stable Eulerian tours with only antiparallel and parallel segments, respectively. The computed data indicates that the variety of stable Eulerian tours becomes relatively large when dealing with objects bigger than the tetrahedron.

Nature Chemical Biology: doi:10.1038/nchembio.1248

Supplementary Table 1 | Number of stable Eulerian tours in the double of some polyhedra. Note that the data for the triangular pyramid supports Theorem 2. The double of none of the first five polyhedra admits a stable Eulerian tour with only parallel segments, the reason being that each of these polyhedra contains vertices of degree 3. On the other hand, in the square bipyramid each vertex is of degree 4 and its double admits 275 stable Eulerian tours with all segments parallel. (**i**) and (**ii**) denote the two defining conditions for stable Eulerian tours and the symbols **A** and **P** indicate that Eulerian tours have only antiparallel and parallel segments, respectively.

Polyhedron	**number of edges**	**(i) + (ii)**	**(i) + (ii) + A**	**(i) + (ii) + P**
triangular pyramid (tetrahedron)	6	3	0	0
square pyramid	8	82	5	0
triangular bipyramid	9	470	0	0
triangular prism	9	25	2	0
square prism (cube)	12	40	0	0
square bipyramid (octahedron)	12	22246	0	275

Nature Chemical Biology: doi:10.1038/nchembio.1248

Supplementary Table 2 | List of the recombinant polypeptide amino acid sequences. Linkers SGPG between peptide segments are underlined. Sequences from vector are double underlined.

Name / peptide sequence	**Amino acid sequence**
TET12 APH-P3-BCR-GCN$_{sh}$-APH-P7-GCN$_{sh}$-P4-P5-P8-BCR-P6	MYHHHHHHSRAGMKQLEKELKQLEKELQAIEKQLAQLQWKAQARKKKLAQLKKKLQASGPGSPEDEIQQLEEEIAQLEQKNAALKEKNQALKYGSGPGDIEQELERAKASIRRLEQEVNQERSRMAYLQTLLAKSGPGQLEDKVEELLSKNYHLENEVARLKKLVGSGPGMKQLEKELKQLEKELQAIEKQLAQLQWKAQARKKKLAQLKKKLQASGPGSPEDEIQALEEKNAQLKQEIAALEEKNQALKYGSGPGQLEDKVEELLSKNYHLENEVARLKKLVGSGPGSPEDKIAQLKQKIQALKQENQQLEEENAALEYGSGPGSPEDENAALEEKIAQLKQKNAALKEEIQALEYGSGPGSPEDKIAQLKEENQQLEQKIQALKEENAALEYGSGPGDIEQELERAKASIRRLEQEVNQERSRMAYLQTLLAKSGPGSPEDKNAALKEEIQALEEENQALEEKIAQLKYGSGTS
TET11 APH-P3-BCR-GCN$_{sh}$-APH-P7-GCN$_{sh}$-P4-P5-P8-BCR	MYHHHHHHSRAGMKQLEKELKQLEKELQAIEKQLAQLQWKAQARKKKLAQLKKKLQASGPGSPEDEIQQLEEEIAQLEQKNAALKEKNQALKYGSGPGDIEQELERAKASIRRLEQEVNQERSRMAYLQTLLAKSGPGQLEDKVEELLSKNYHLENEVARLKKLVGSGPGMKQLEKELKQLEKELQAIEKQLAQLQWKAQARKKKLAQLKKKLQASGPGSPEDEIQALEEKNAQLKQEIAALEEKNQALKYGSGPGQLEDKVEELLSKNYHLENEVARLKKLVGSGPGSPEDKIAQLKQKIQALKQENQQLEEENAALEYGSGPGSPEDENAALEEKIAQLKQKNAALKEEIQALEYGSGPGSPEDKIAQLKEENQQLEQKIQALKEENAALEYGSGPGDIEQELERAKASIRRLEQEVNQERSRMAYLQTLLAKSGTS
TET12Scr GCN$_{sh}$-APH-APH-P3-BCR-P7-GCN$_{sh}$-P4-P5-P8-BCR-P6	MYHHHHHHSRAGQLEDKVEELLSKNYHLENEVARLKKLVGSGPGMKQLEKELKQLEKELQAIEKQLAQLQWKAQARKKKLAQLKKKLQASGPGMKQLEKELKQLEKELQAIEKQLAQLQWKAQARKKKLAQLKKKLQASGPGSPEDEIQQLEEEIAQLEQKNAALKEKNQALKYGSGPGDIEQELERAKASIRRLEQEVNQERSRMAYLQTLLAKSGPGSPEDEIQALEEKNAQLKQEIAALEEKNQALKYGSGPGQLEDKVEELLSKNYHLENEVARLKKLVGSGPGSPEDKIAQLKQKIQALKQENQQLEEENAALEYGSGPGSPEDENAALEEKIAQLKQKNAALKEEIQALEYGSGPGSPEDKIAQLKEENQQLEQKIQALKEENAALEYGSGPGDIEQELERAKASIRRLEQEVNQERSRMAYLQTLLAKSGPGSPEDKNAALKEEIQALEEENQALEEKIAQLKYGSGTS
TET12SplitYFP **CYFP-** APH-P3-BCR-GCN$_{sh}$-APH-P7-GCN$_{sh}$-P4-P5-P8-BCR-P6-**NYFP**	MYHHHHHHSRAGDKQKNGIKVNFKIRHNIEDGSVQLADHYQQNTPIGDGPVLLPDNHYLSYQSALSKDPNEKRDHMVLLEFVTAAGITLGMDELYKSGSGMKQLEKELKQLEKELQAIEKQLAQLQWKAQARKKKLAQLKKKLQASGPGSPEDEIQQLEEEIAQLEQKNAALKEKNQALKYGSGPGDIEQELERAKASIRRLEQEVNQERSRMAYLQTLLAKSGPGQLEDKVEELLSKNYHLENEVARLKKLVGSGPGMKQLEKELKQLEKELQAIEKQLAQLQWKAQARKKKLAQLKKKLQASGPGSPEDEIQALEEKNAQLKQEIAALEEKNQALKYGSGPGQLEDKVEELLSKNYHLENEVARLKKLVGSGPGSPEDKIAQLKQKIQALKQENQQLEEENAALEYGSGPGSPEDENAALEEKIAQLKQKNAALKEEIQALEYGSGPGSPEDKIAQLKEENQQLEQKIQALKEENAALEYGSGPGDIEQELERAKASIRRLEQEVNQERSRMAYLQTLLAKSGPGSPEDKNAALKEEIQALEEENQALEEKIAQLKYGSGSGVSKGEELFTGVVPILVELDGDVNGHKFSVSGEGEGDATYGKLTLKFICTTGKLPVPWPTLVTTFGYGLQCFARYPDHMKQHDFFKSAMPEGYVQERTIFFKDDGNYKTRAEVKFEGDTLVNRIELKGIDFKEDGNILGHKLEYNYNSHNVYIMASGTS
TET11SplitYFP **CYFP-** APH-P3-BCR-GCN$_{sh}$-APH-P7-GCN$_{sh}$-P4-P5-P8-BCR -**NYFP**	MYHHHHHHSRAG**DKQKNGIKVNFKIRHNIEDGSVQLADHYQQNTPIGDGPVLLPDNHYLSYQSALSKDPNEKRDHMVLLEFVTAAGITLGMDELYK**SGSGMKQLEKELKQLEKELQAIEKQLAQLQWKAQARKKKLAQLKKKLQASGPGSPEDEIQQLEEEIAQLEQKNAALKEKNQALKYGSGPGDIEQELERAKASIRRLEQEVNQERSRMAYLQTLLAKSGPGQLEDKVEELLSKNYHLENEVARLKKLVGSGPGMKQLEKELKQLEKELQAIEKQLAQLQWKAQARKKKLAQLKKKLQASGPGSPEDEIQALEEKNAQLKQEIAALEEKNQALKYGSGPGQLEDKVEELLSKNYHLENEVARLKKLVGSGPGSPEDKIAQLKQKIQALKQENQQLEEENAALEYGSGPGSPEDENAALEEKIAQLKQKNAALKEEIQALEYGSGPGSPEDKIAQLKEENQQLEQKIQALKEENAALEYGSGPGDIEQELERAKASIRRLEQEVNQERSRMAYLQTLLAKSGSG**VSKGEELFTGVVPILVELDGDVNGHKFSVSGEGEGDATYGKLTLKFICTTGKLPVPWPTLVTTFGYGLQCFARYPDHMKQHDFFKSAMPEGYVQERTIFFKDDGNYKTRAEVKFEGDTLVNRIELKGIDFKEDGNILGHKLEYNYNSHNVYIMA**SGTS

Nature Chemical Biology: doi:10.1038/nchembio.1248

Supplementary Figures 4-11

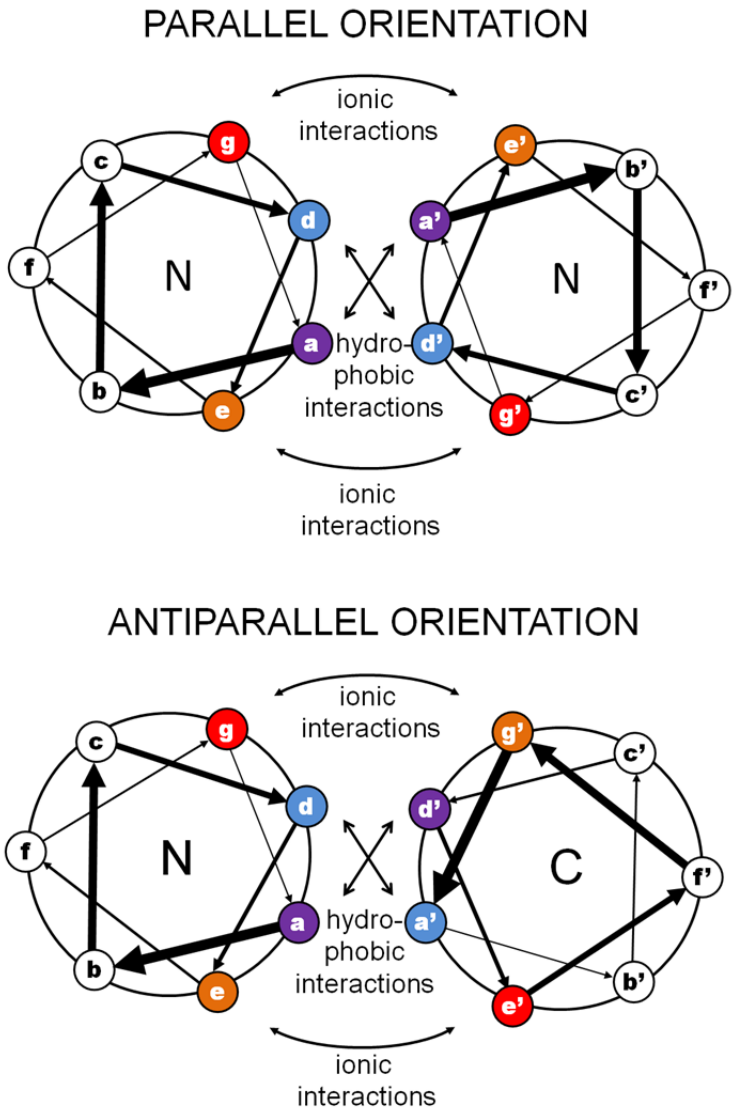

Supplementary Figure 4 | Helical wheel diagram for parallel and antiparallel coiled-coil dimers. The sequence of seven amino acid residues (heptad repeat) is denoted by positions ***abcdefg***. Positions ***a*** and ***d*** are typically occupied by hydrophobic residues forming a hydrophobic core. Positions ***e*** and ***g*** are frequently occupied by charged residues that by the formation of interhelical electrostatic interactions direct the parallel or antiparallel helix orientation. Stabilizing interactions between residues of the two helices are denoted by arrows.

Nature Chemical Biology: doi:10.1038/nchembio.1248

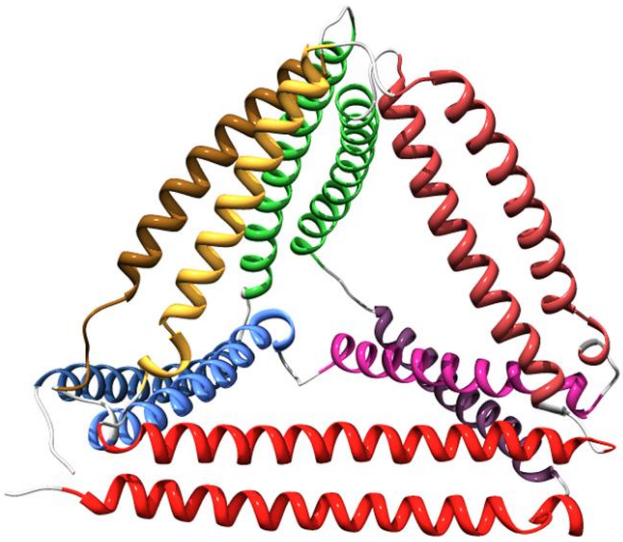

Supplementary Figure 5 | Molecular model of the folded tetrahedron TET12. The model was prepared by using the MODELLER[33] program as described in the online methods section. Scale bar below the model indicates 5 nm.

Nature Chemical Biology: doi:10.1038/nchembio.1248

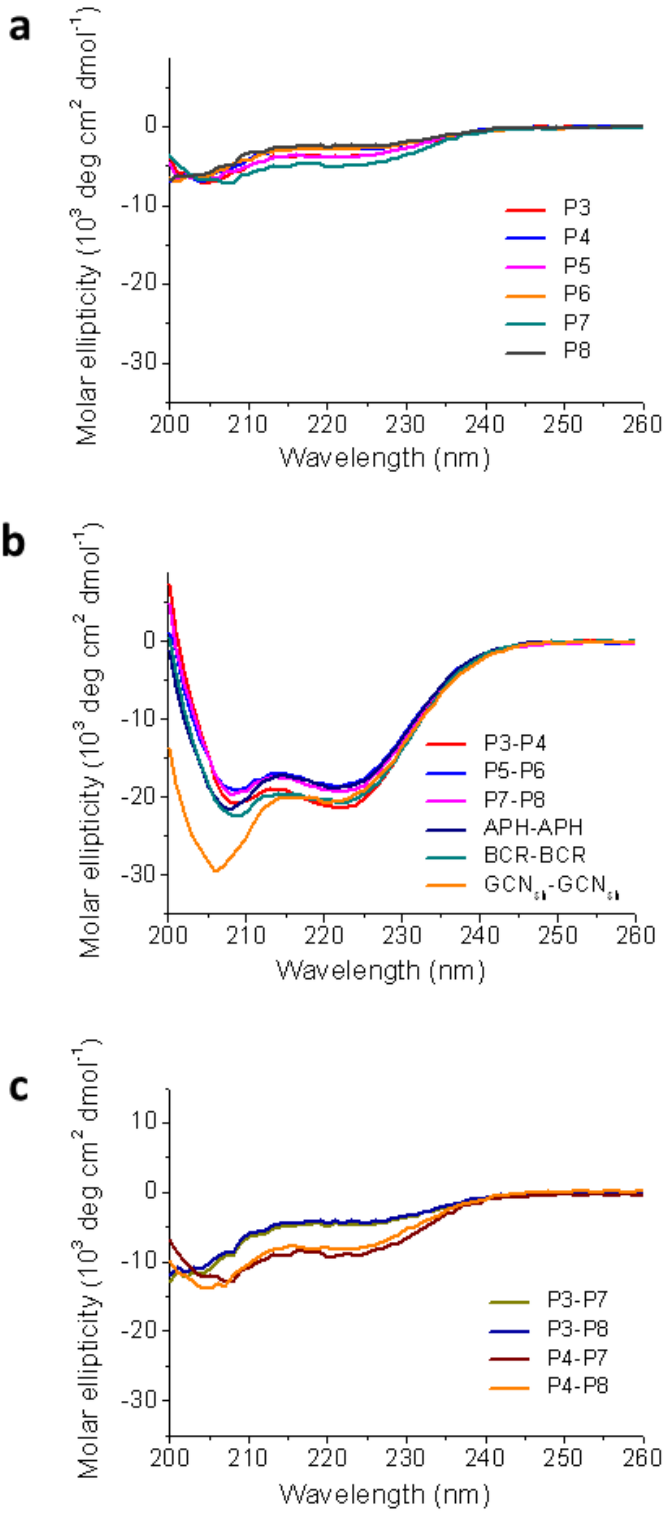

Supplementary Figure 6 | Analysis of the orthogonality of the designed coiled-coil pair combinations used for the construction of the tetrahedron. CD spectra of synthetic peptides (**a**), orthogonal peptide pairs (**b**) or non-orthogonal peptide pairs (**c**) at concentration of 25 μM in 20 mM Tris, pH 8.0, were recorded at 20°C. Spectra are the average of three scans.

Nature Chemical Biology: doi:10.1038/nchembio.1248

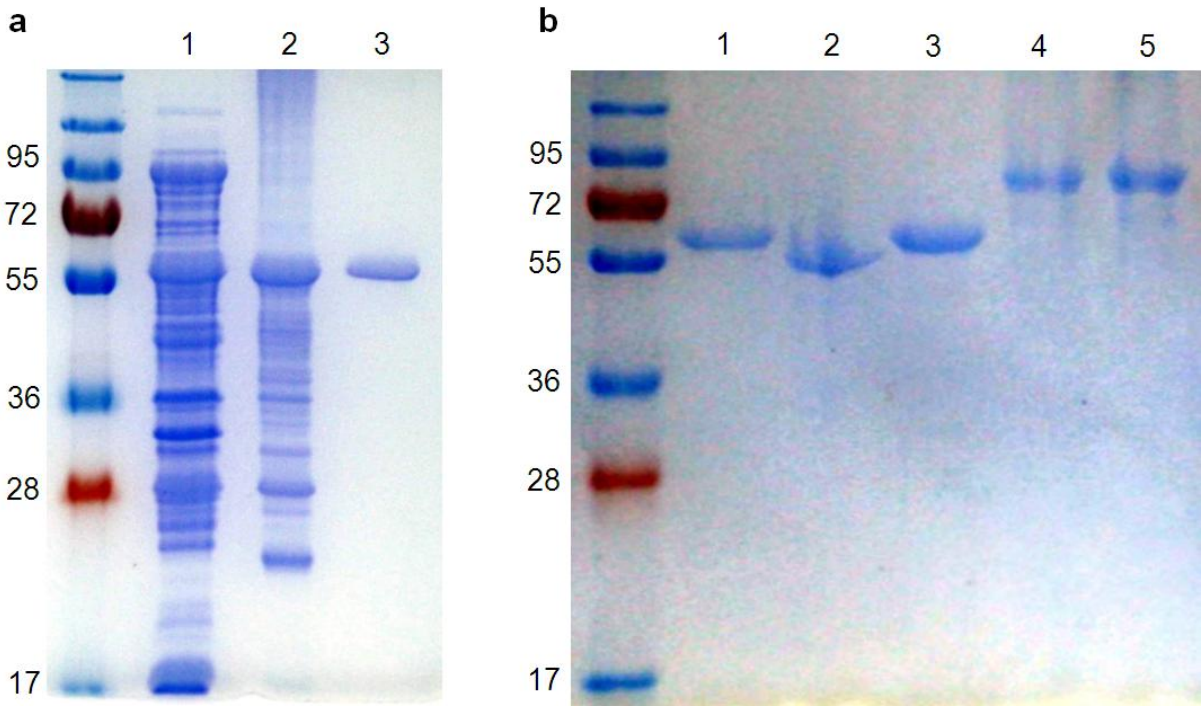

Supplementary Figure 7 | Purification of polypeptides TET12, TET12splitYFP, variants with deleted (TET11) and scrambled (TET12scr) segment order. (**a**) Polypeptide TET12 (M_w = 53,391 Da) was expressed in the form of inclusion bodies (1), which were purified by chelating chromatography (2) and RP-HPLC (3). (**b**) SDS-PAGE of the purified polypeptides TET12 (1), TET11 (M_w = 49,381 Da) (2), TET12scr (M_w = 53,391 Da) (3), TET12splitYFP (M_w = 80,810 Da) (4) and TET11splitYFP (M_w = 76,800 Da) (5). SDS-PAGE was performed on a 12 % separation gel under non-reducing conditions and proteins were stained with a solution of Coomassie brilliant blue R (Sigma).

Nature Chemical Biology: doi:10.1038/nchembio.1248

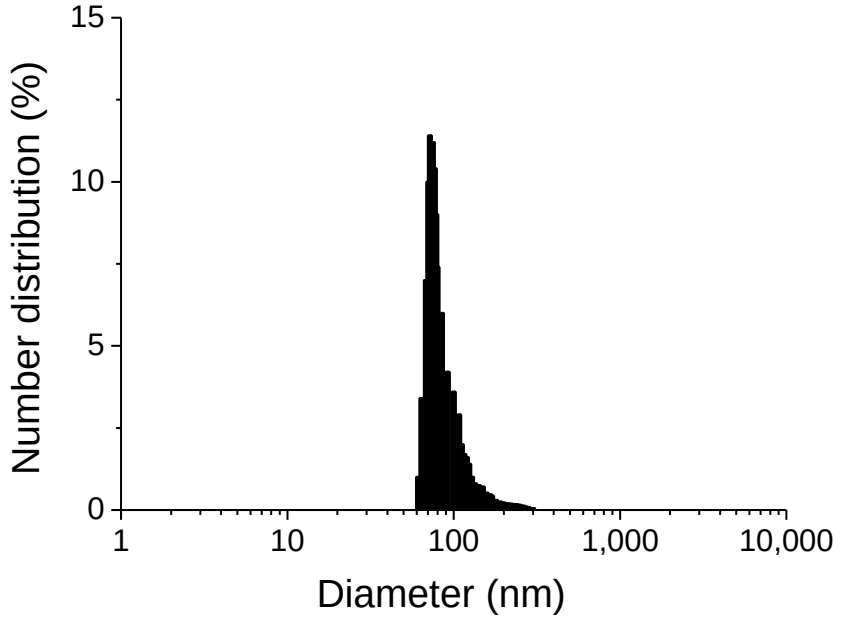

Supplementary Figure 8 | Formation of aggregates produced by dialysis at high, 10 μM TET12 polypeptide concentration. The hydrodynamic diameters above 80 nm were determined by DLS in three independent experiments with the calculated mean value ± s.d. of 100.2 ± 20.4 nm. Representative histogram of one experiment is shown.

Nature Chemical Biology: doi:10.1038/nchembio.1248

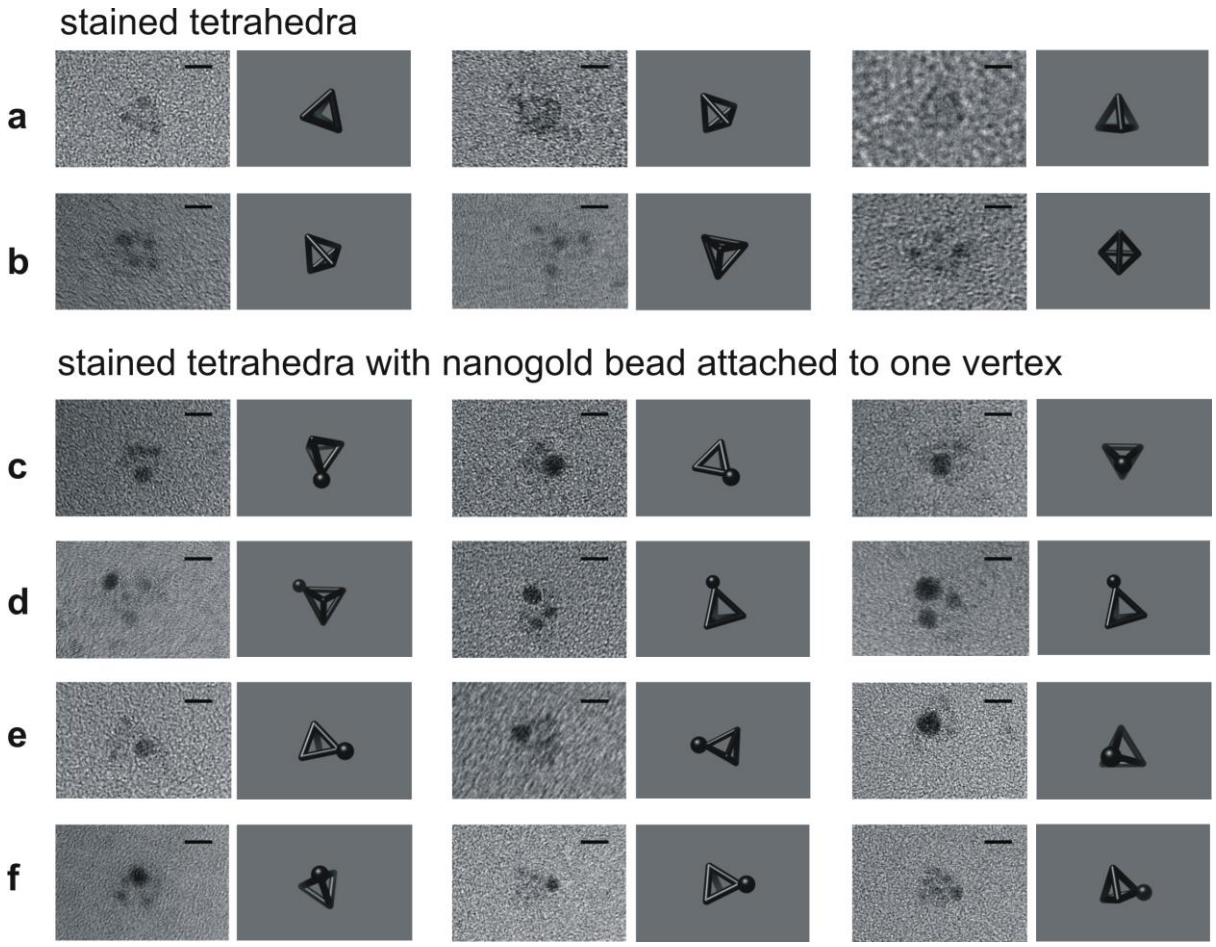

Supplementary Figure 9 | Tetrahedral particles visualized by TEM. Samples of self-assembled polypeptide tetrahedra were either stained with uranyl (**a,b**) or uranyl staining was used after 1.8-nm nanogold beads were bound to one vertex of the tetrahedron via $(His)_6$ peptide tag (**c-f**). Self-assembling procedures were performed by slow refolding of denatured polypeptide TET12. The samples were positively stained using either a short time (**a**) or a long time (**b**) staining procedure. Tetrahedral structures were obtained by slow refolding of chemically denatured polypeptide (**c,d**) or by slow annealing of temperature denatured polypeptide TET12 (**e**). Polypeptide structures were labeled by nanogold and subsequently stained with uranyl, for a short time (**c,e**) or a long time (**d**). (**f**) TET12splitYFP formed tetrahedral structures. Scale bars, 5 nm.

Nature Chemical Biology: doi:10.1038/nchembio.1248

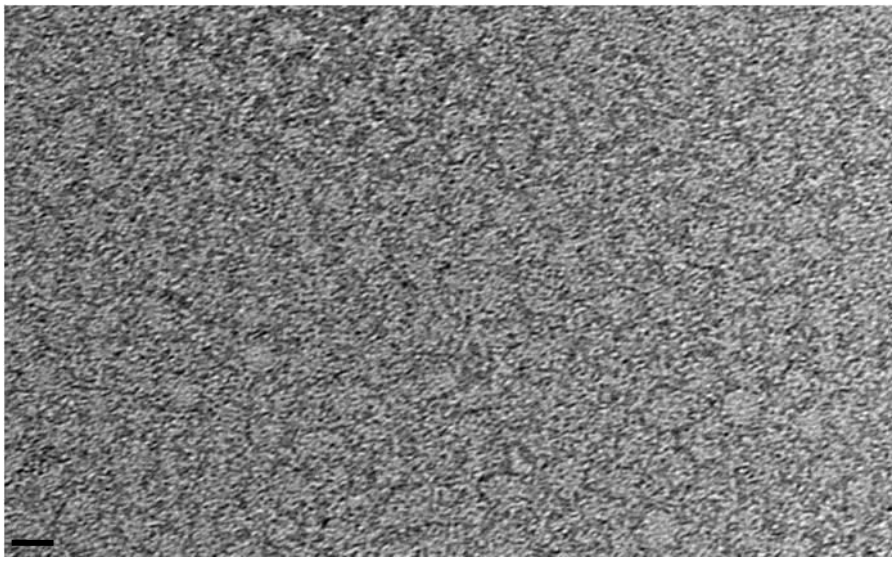

Supplementary Figure 10 | Self-assembly of TET12 at high concentration forms a network rather than discrete structures. TET12 was dialyzed at high concentration (10 μM) from 6 M GdnHCl against 20 mM Tris buffer, pH 8.5 and 150 mM NaCl. Sample was imaged by TEM using uranyl staining. Self-assembly at high concentration reveals the formation of network due to intermolecular interactions with the complementary segments from the other molecules. Scale bar, 20 nm.

Nature Chemical Biology: doi:10.1038/nchembio.1248

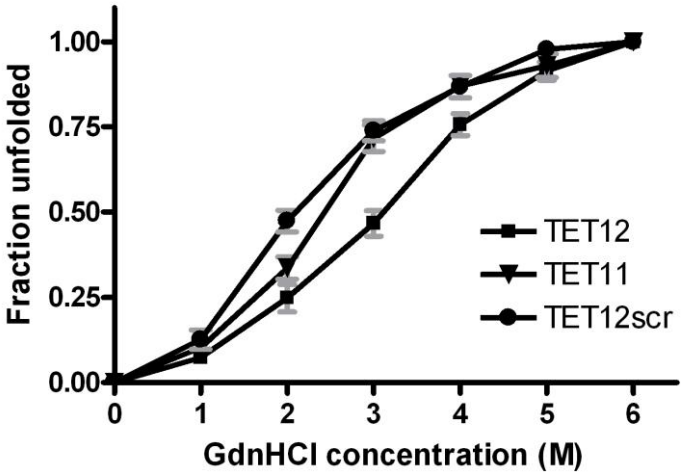

Supplementary Figure 11 | Decreased stability of structures formed by TET12 variants with incomplete (TET11) or scrambled (TET12scr) coiled-coil-building segments in comparison to TET12 nanostructures. Stability of the assembled material at low, 100 nM polypeptide concentration followed by concentration of samples to 4 μM was determined from the dependence of the molar ellipticity at 222 nm in addition of GdnHCl from 0 to 6 M. Values are expressed as means of triplicate measurements. Error bars indicate the s.d. of the measurements.

Nature Chemical Biology: doi:10.1038/nchembio.1248